

Development of an Imaging System for an Electron Spectrometer for laser-accelerated electrons

Vitória Macedo Costa Brandão
 IPEN – CNEN
 São Paulo, SP, Brazil
 vik.mbrandao@gmail.com

Ricardo E. Samad
 IPEN – CNEN
 São Paulo, SP, Brazil
 orcid.org/0000-0001-7762-8961

Abstract—We present the results of an electron spectrometer with an imaging system to determine the energy spectrum of laser accelerated electrons. The spectrometer is composed by a region with a constant magnetic field that deflects relativistic electrons according to their kinetic energy, and a luminescent screen into which the electrons impinge. The imaging system optimizes the collection of the screen luminescence, which is inside a vacuum chamber, and magnifies it, through a window, into a CCD in atmosphere that records the light pattern, from which the energy spectrum is recovered.

Keywords— *Imaging System, electron spectrometer, laser wakefield acceleration.*

I. INTRODUCTION

Laser wakefield acceleration (LWFA) was introduced in 1979 by Tajima and Dawson [1] and is a method to accelerate electrons in laser created plasmas that support acceleration gradients three orders of magnitude higher than conventional RF accelerators [2]. This extremely high gradients can decrease the acceleration length by a 10^3 factor, allowing the generation of GeV electron beams in tens of centimeters [3]. When relativistic intensities ultrashort laser pulses are focused on a gas target, ionization occurs and the relativistic ponderomotive force creates a plasma with a periodic charge distribution, expelling electrons from the laser axis, generating waves of charge density that propagate through the plasma at nearly the pulse speed [4, 5]. This density modulation creates longitudinal electric fields that can reach TV/m, accelerating electrons forward.

To characterize the laser accelerated electrons energy, electron spectrometers have been developed [6]. The basic setup of this kind of spectrometer is represented in Fig. 1: a slit blocks most of the laser beam and selects low divergence electrons, which traverse a constant magnetic field region and are deflected by the Lorentz force according to their energy.

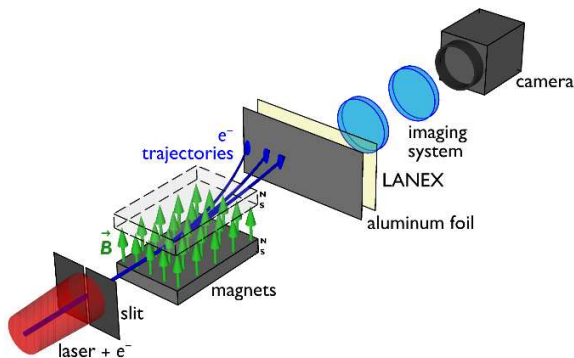


Fig. 1. Electron spectrometer scheme. The electrons are deflected by the magnetic field and hit a scintillator (LANEX), whose emission is registered by a CCD camera.

When the electrons go through the constant field region, they follow a curved path with the Larmor radius [7], which deflects them depending on their energy. For relativistic electrons, we could determine that the transversal deviation, in cm, from their original propagation direction is given by:

$$\delta y(E) = \sqrt{4 \left(0.33 \frac{E}{B}\right)^2 \sin^2\left(\frac{1}{2} \sin^{-1}\left(\frac{LB}{0.33E}\right)\right)^2 - L^2} \quad (1)$$

where E is the electron energy in MeV, B is the magnetic field in T, and L is the length of the constant magnetic field in cm.

After being deflected, the electrons hit a luminescent screen (behind an aluminum foil that blocks the remaining laser light), which is imaged on a CCD camera that records the electrons positions, from which their energy spectrum can be recovered.

Fig. 2 presents the luminescence intensity distribution produced by a spectrometer with $B=0.6$ T and $L=5$ cm, obtained by applying (1) to the simulated energy spectrum [8] shown in the inset. The spectrometer field and length were chosen to characterize the energy peak around 17 MeV and disregard the low energy electrons. It can be seen that the electrons at the exit of the constant B region are transversally spread across ~ 3 cm, and this whole distribution has to be imaged on the CCD surface.

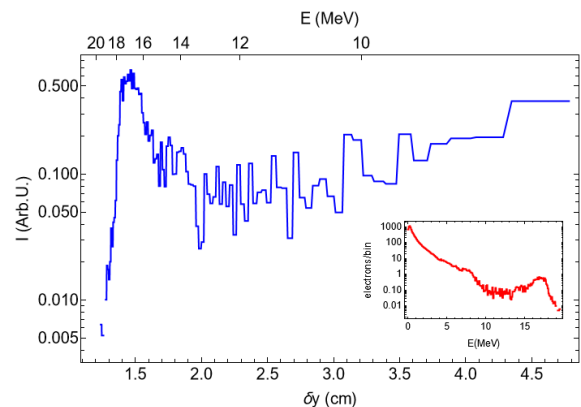


Fig. 2. Luminescent intensity distribution (transversal electron displacement) for the electrons energy spectrum shown in the inset, with 0.1 MeV bins.

Our research group is working to implement a laser electron facility at the Nuclear and Energy Research Institute (IPEN) [9], and this work presents the theoretical development of imaging systems to project the emission of the LANEX screen onto a CCD camera.

II. METHODOLOGY

Fig. 3 presents the basic setup of the electron spectrometer imaging system that will be built in our laboratory, inside a 50 cm in diameter vacuum chamber. The spectrometer

This work was supported by FAPESP, CNPq and CAPES grants.

(magnets not shown) is placed after the electron acceleration region, as is the LANEX screen. The CCD active element usually has a ~ 10 mm dimension, so the LANEX emission region, which is a few centimeters wide (Fig. 1), must be demagnified by $\sim 1/10$ by the imaging system to be captured by the camera. Also, the collecting lens should be as close as possible to the LANEX and have a big diameter to maximize the light collecting solid angle (effective Numerical Aperture - NA) to increase the luminosity of the real image projected at the CCD, while reducing its noise-to-signal-ratio (NSR). Care must be taken with large lenses to minimize spherical and chromatic aberrations, which would degrade the image, leading to uncertainties in the electrons energy determination. This approach is advantageous over using a commercial objective to project the image onto the CCD, since that objective would be placed outside the vacuum chamber, resulting in a small effective NA, decreasing the light collection and increasing the NSR.

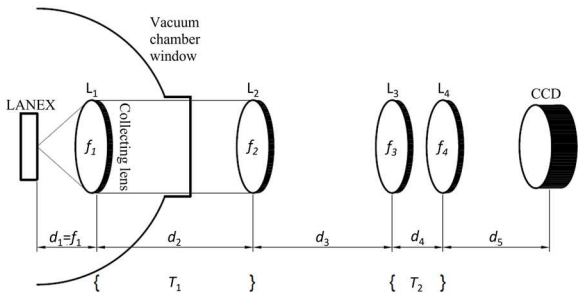


Fig. 3. Scheme of the electron spectrometer imaging system.

A single lens cannot generate a demagnified real image; a telescope composed by two lenses with foci f_1 and f_2 separated by $f_1 + f_2$ produces a real image with magnification f_2/f_1 , meaning that a long lens must be used to collect the LANEX emission, decreasing the effective NA and the light collection. These restrictions led us to consider using an imaging system composed by two telescopes, as indicated in Fig. 3. The first one, composed by lenses L_1 and L_2 transports the LANEX image to the outside of the vacuum chamber, and the second one (L_3 and L_4) projects this image, demagnified, on the CCD.

To study the imaging system, we built its ray transfer matrix (ABCD matrix [10]) considering the distances and foci shown in Fig. 3. Setting the matrix element $B = 0$ determines the final image position, and using this condition in the matrix element A returns the system magnification m .

III. RESULTS

Determining the telescope parameters from the matrix elements A and B is not a simple task due to the large number of variables (5 distances 4 foci, and magnification) that can be chosen, so we imposed restrictions on the system design:

1. Lens L_1 has $f_1 = 5$ cm, and the LANEX screen is at its focus ($d_1 = 5$ cm), maximizing light collection and collimating the beam with a lens with low aberration;
2. Lens L_2 has $f_2 = f_1 = 5$ cm, and d_2 can have any value due to the collimated beam (condition 1 above), producing an image with magnification -1;
3. Lens L_3 has $f_3 = 5$ cm.

The established conditions still leave f_4 , d_3 and d_4 to be determined. We observed that setting $d_3 > f_3$ produces the demagnified final image. We chose $f_3 = 20$ cm, resulting in:

$$m = f_4 / (15 - 2 d_4 + 2 f_4), \quad (2)$$

$$d_5 = f_4 (2 d_4 - 15) / (2 d_4 - 2 f_4 - 15), \quad (3)$$

which determine the magnification m and image position d_5 of the imaging system. Many combinations are possible, but considering the lenses available in our laboratory and the magnification shown in Fig. 4 as a function of L_3 and L_4 separation, a good choice is $f_4 = 3$ cm (an achromatic doublet, to decrease aberration for such a short focus), and $d_4 = 1.5$ cm, which result in $m = 0.17$, and $d_5 = 2$ cm, fulfilling our needs to project the image on the CCD. This is a preliminary calculation that will be refined along with the assembly and performance testing of the imaging system.

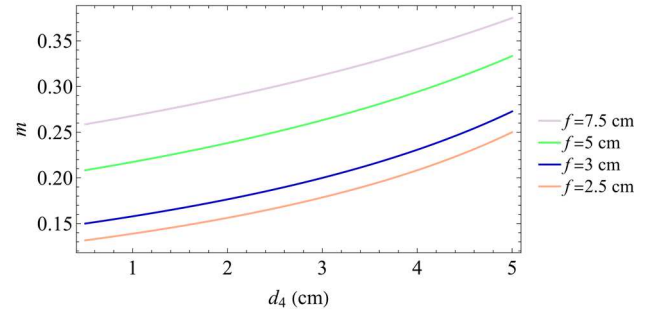


Fig. 4. Imaging system magnification as a function of the separation between lenses L_3 and L_4 , for 4 different lenses.

IV. CONCLUSIONS

We designed an imaging system that transports the luminescence pattern generated by laser accelerated electrons on a LANEX scintillator inside a vacuum chamber, to a camera outside it, demagnifying the image to fit on the CCD surface. The ray transfer matrix of the system allowed determining the optical parameters of the imaging system. More studies are necessary to obtain an optimal solution that maximizes the light collection, minimizing aberrations.

REFERENCES

- [1] T. Tajima, and J. M. Dawson, "Laser Electron Accelerator," Physical Review Letters, vol. 43, pp. 267-270, 1979.
- [2] H. Kim, "Multi-GeV Laser Wakefield Electron Acceleration with PW Lasers," Applied Sciences, vol. 11, p. 5831, 2021.
- [3] W. P. Leemans, "GeV electron beams from a centimetre-scale accelerator," Nature Physics, vol. 2, pp. 696-699, 2006.
- [4] J. Faure, "A laser-plasma accelerator producing monoenergetic electron beams," Nature, vol. 431, pp. 541-544, 2004.
- [5] E. Esarey, C. B. Schroeder, and W. P. Leemans, "Physics of laser-driven plasma-based electron accelerators," Reviews of Modern Physics, vol. 81, pp. 1229-1285, 2009.
- [6] K. V. Gubin, Y. I. Mal'tseva, A. V. Ottmar, and T. V. Rybitskaya, "A Spectrometer for Measuring the Characteristics of a Single Laser-Accelerated Electron Bunch with a Small Charge," Instruments and Experimental Techniques, vol. 63, pp. 325-333, 2020.
- [7] F. Chen, Introduction to Plasma Physics and Controlled Fusion, 3rd ed. Heidelberg: Springer International Publishing, 2016.
- [8] E. P. Maldonado, "Study of quasimonoenergetic electron bunch generation in self-modulated laser wakefield acceleration using TW or sub-TW ultrashort laser pulses," AIP Advances, vol. 11, p. 065116, 2021.
- [9] N. D. Vieira, "Laser wakefield electron accelerator: possible use for radioisotope production," 2021 SBFoton International Optics and Photonics Conference (SBFoton IOPC), São Carlos, SP, Brazil (virtual), 2021.
- [10] F. A. Jenkins, and H. E. White, Fundamentals of optics, 4th ed. New York: McGraw-Hill, 2001.